Incoherent Ellipsometry of Wide and Moderate Gap Materials

Yonggu Shim[1] and Nazim Mamedov[2]

[1] *Graduate School of Engineering, Osaka Prefecture University, Osaka, Japan*

[2] *Institute of Physics, National Academy of Sciences of Azerbaijan, Baku, Azerbaijan*

Outline

I. Ellipsometry of moderate and wide gap materials
II. Conventional ellipsometry on non-depolarizing samples (biaxial $CaGa_2S_4$)
III. Incoherent ellipsometry on depolarizing samples ($TlMeX_2$)
IV. Summary of this presentation

I. Ellipsometry of Moderate and Wide Gap Materials

- Ellipsometric angles ϕ and Δ
- Stokes parameters and different ellipsometer types
- Light source and sample configuration based classification of ellipsometers
- Information obtained by using ellipsometry
- Analytical methods and approaches
- Some examples of technical (multilayer profile) and physical (electronic band structure) ellipsometric applications

Ellipsometric angles ϕ and Δ

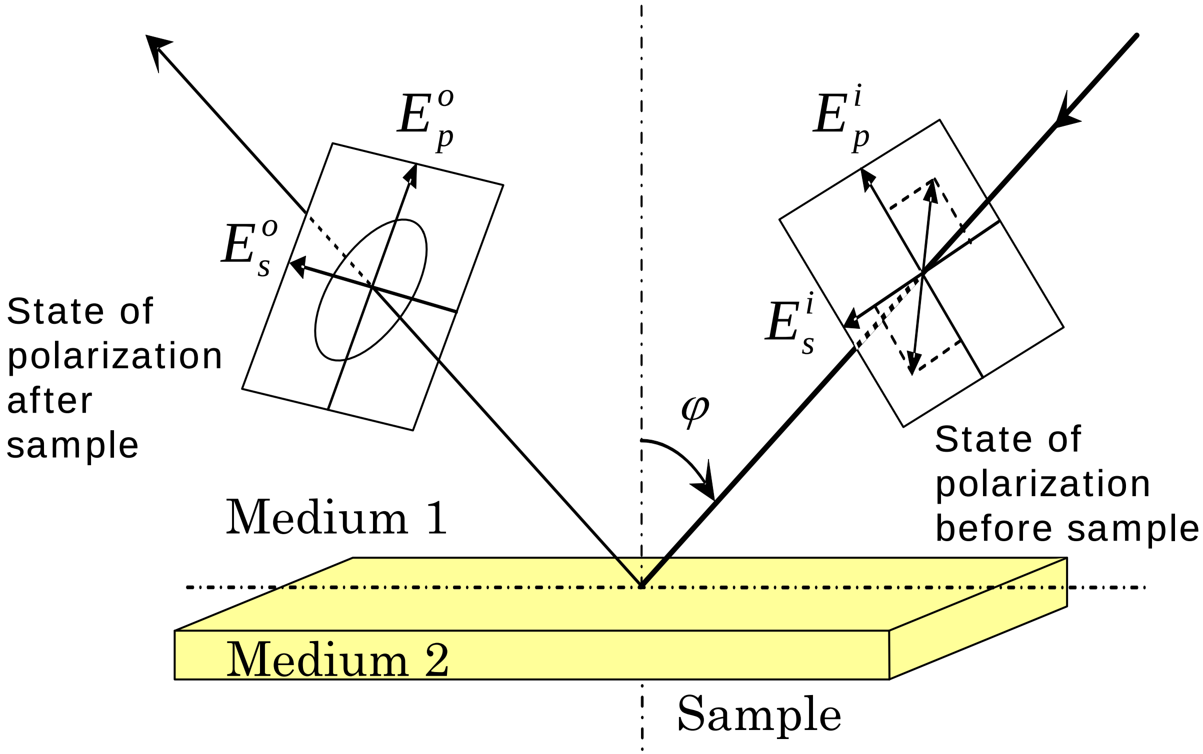

Schematic diagram of ellipsometric measurement.

$$\frac{r_{pp}}{r_{ss}} = \frac{\dfrac{E_p^o}{E_p^i}}{\dfrac{E_s^o}{E_s^i}} = \tan\psi \cdot e^{i\Delta}$$

Fresnel reflection coefficients

$$r_{pp} = \frac{\tilde{n}_2^{\,2}\cos\varphi - \tilde{n}_1\sqrt{\tilde{n}_2^{\,2} - \tilde{n}_1^{\,2}\sin^2\varphi}}{\tilde{n}_2^{\,2}\cos\varphi + \tilde{n}_1\sqrt{\tilde{n}_2^{\,2} - \tilde{n}_1^{\,2}\sin^2\varphi}}$$

$$r_{ss} = \frac{\tilde{n}_1\cos\varphi - \sqrt{\tilde{n}_2^{\,2} - \tilde{n}_1^{\,2}\sin^2\varphi}}{\tilde{n}_1\cos\varphi + \sqrt{\tilde{n}_2^{\,2} - \tilde{n}_1^{\,2}\sin^2\varphi}}$$

Ellipsometry measures the change of the polarization state of the light reflected (transmitted) by a sample. This change is described by ellipsometric parameter Ψ and Δ. These values are related to the ratio of Fresnel reflection coefficients. The complex refractive indices are determined from measured Ψ and Δ.

Stokes parameters and different ellipsometer types

Stokes parameters

$$S = \begin{pmatrix} S_0 \\ S_1 \\ S_2 \\ S_4 \end{pmatrix} = \begin{pmatrix} I_r \\ I_s - I_p \\ I_{45} - I_{-45} \\ I^{+} - I^{-} \end{pmatrix} = \begin{pmatrix} 1 \\ -\alpha \\ \beta \\ -\gamma \end{pmatrix} I_r$$

- I_r : the total intensity of the light.
- I_s and I_p : s- and p-polarized components.
- I_{+45} and I_{-45} : intensity for an angle of polarization of $\pm 45^\circ$.
- I^+ and I^- : intensity for left- and right-polarized light.

Degree of polarization

$$P = \sqrt{\alpha^2 + \beta^2 + \gamma^2}$$

$P=1$: Totally polarized light
$P<1$: Depolarized light

<u>Depolarization effect in SE measurement</u>

- Sample with large surface roughness.
- Transparent region of parallel plate sample.
- Inhomogeneous material.

For perfect ellipsometric analysis → Measurement for all Stokes parameters – (Full Optical Experiment)

Stokes parameters and different ellipsometer types

Classification by configurations of optical components

- Null Ellipsometer (NE)
- Rotating-Analyzer Ellipsometer (RAE)
- Phase-Modulation Ellipsometer (PME)
- Rotating-Compensator Ellipsometer (RCE)

Measurement system (development year)	Measured parameters	Measurable region	Main characteristic
NE (1945)	S_0, S_1, S_2, S_3	$0° \leqq \Psi \leqq 90°$ $-180° < \Delta \leqq 180°$	high accuracy, long measurement time
RAE (1975)	S_0, S_1, S_2	$0° \leqq \Psi \leqq 90°$ $0° \leqq \Delta \leqq 180°$	simple optical configuration, wide measurable wavelength region, measurement time (1ms), S_3 parameter
PME(1982)	S_0, S_1, S_3	$0° \leqq \Psi \leqq 90°$ $0° \leqq \Delta \leqq 180°$	high speed measurement (20 μs), all S parameter by changing optical configuration
	S_0, S_2, S_3	$0° \leqq \Psi \leqq 45°$ $-180° < \Delta \leqq 180°$	
RCE(1998)	S_0, S_1, S_2, S_3	$0° \leqq \Psi \leqq 90°$ $-180° < \Delta \leqq 180°$	simultaneous measurement of all S parameter, measurement time (1ms), complex correction procedure

Light source and sample configuration based classification of ellipsometers

Light source

- **Single-Wavelength Ellipsometer (SWE)**
  employing a laser (lasers) in order to have a high-intensity small-spot probe-beam for high resolution imaging ellipsometry

- **Spectroscopic Ellipsometer (SE)**
  employing an incoherent light source to provide continuous access to the wavelengths and high accuracy of the obtained data

Sample configuration

- **Reflection ellipsometer**
  Measurements on materials with strong absorption

- **Transmission ellipsometer (Polarimeter)**
  Measurements on transparent or weakly absorbing materials

Information obtained by using ellipsometry

Characterization of thin films

- Thickness
- Depth profile
- Surface roughness
- Contaminant layer
- Oxide overlayer

Spectroscopic Ellipsometry

Optical constants

- Refractive indices
- Absorption coefficient
- Dielectric function

Material properties

- Composition
- Doping
- Surface temperature
- Surface morphology

Analytical methods and approaches

Construction of optical model

Selection of dispersion model

Ellipsometric measurement to obtain ϕ and Δ

Calculation of error function

Regression process to minimize error function

We can determine the optical constants (refractive index, dielectric function), film thickness, surface roughness…

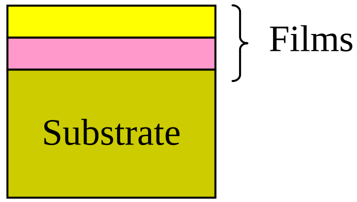

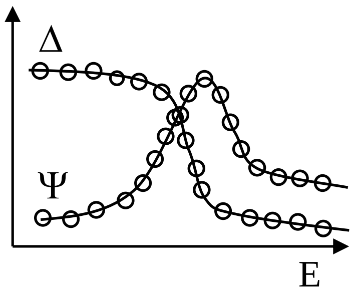

$$\sigma^2 = \sum_{j=1}^{M} \{\rho_{ex}(\hbar\omega_j) - \rho_{cal}(\hbar\omega_j)\}^2$$

$$\rho = \frac{r_{pp}}{r_{ss}} = \tan\Psi \exp(i\Delta)$$

A technical application

Analysis of multi-layer structure*

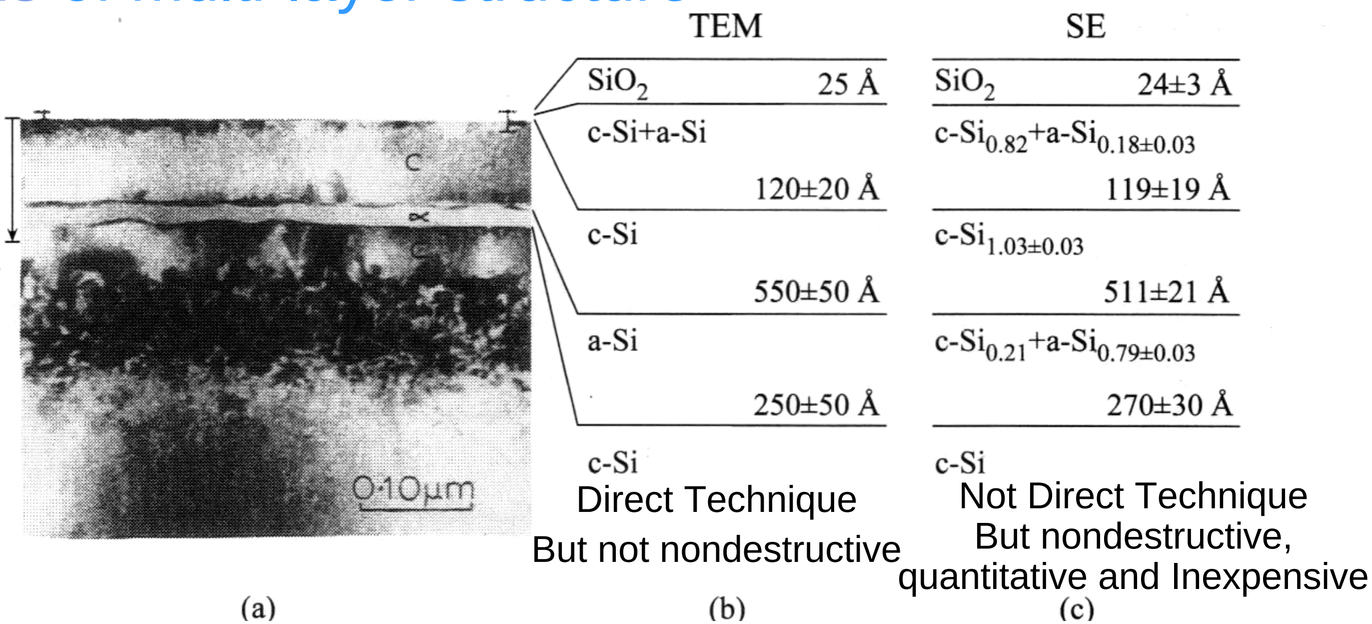

Comparison of cross-section transmission electron microscopy and spectroscopic ellipsometry for depth profiling. (a) cross-section TEM micrograph of sample; (b) schematic diagram of model for the samples as evaluated from TEM; (c) schematic diagram of model for the sample as evaluated from SE.

*K.Vedam: Thin Solid Films **313-314** (1998) 1.

A physical application

Analysis of band structure*

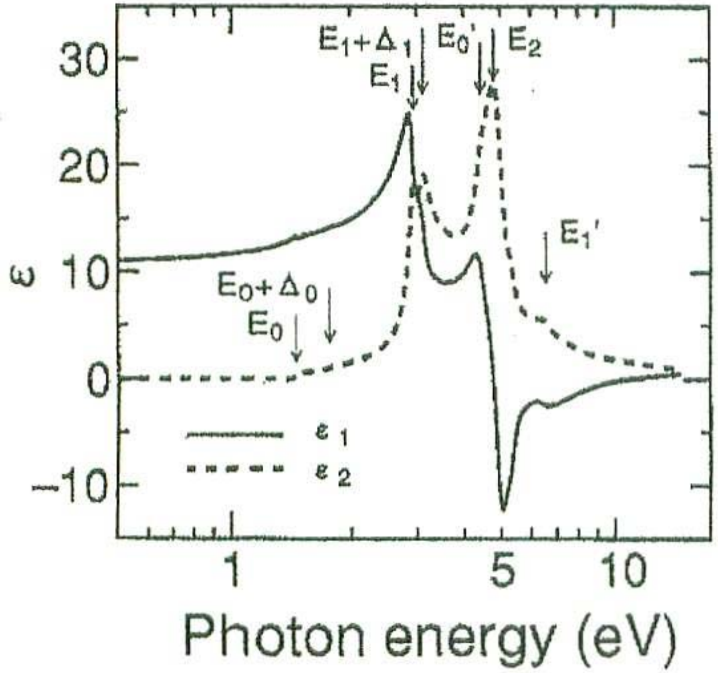

Dielectric function spectra of GaAs

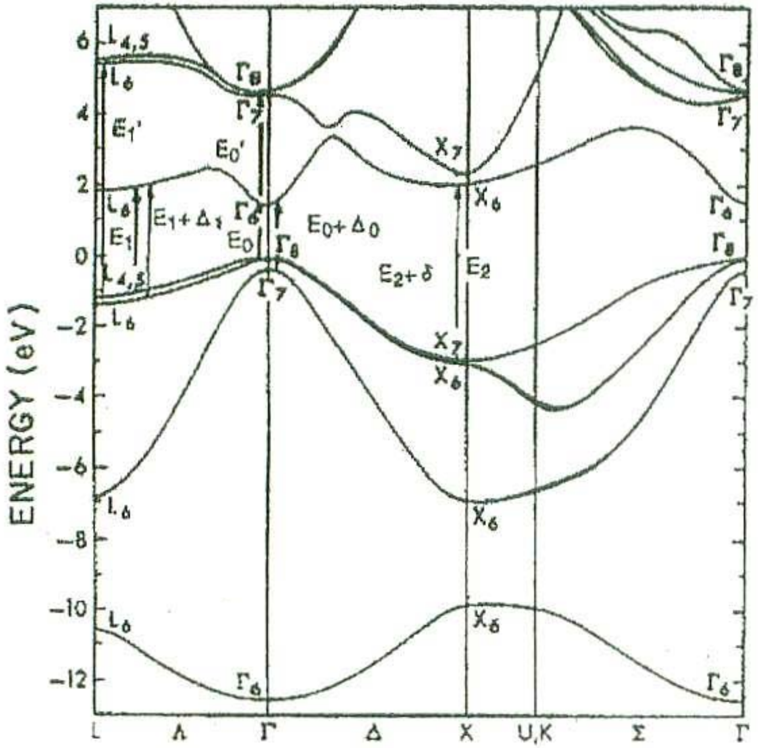

Band structure of GaAs

Using SE measurement, We can obtain Information on band structure from analyses of dielectric function spectra.

*S. Adachi: *GaAs and Related Materials: Bulk Semiconducting and Superlattice properties*, World Scientific Pub. Co. Inc. (1994).

II. Conventional ellipsometry on non-depolarizing samples (biaxial $CaGa_2S_4$)

- Background
- Structure and symmetry of CGS ($CaGa_2S_4$)
- Strategy for determination of optical constants of biaxial CGS by using only (100) plane
- Polarized transmission intensity (PTI) – an auxiliary to SE below the energy gap of novel materials
- Above energy gap SE of CGS
- Summary on CGS

Background

- Orthorhombic wide-gap ternary semiconductor $CaGa_2S_4$ (CGS) is already regarded as promising host to rare earth Ce^{3+} (2.64eV: 470nm) and Eu^{2+}(2.23eV: 555nm) to apply in flat panel displays and lasers. For such applications, the photon energy of the utilized light lies in visible, blue-to-red or infrared spectral range, being smaller than energy gap (~4.10eV) of the material.
- The correct information on optical constants of single crystalline CGS is required for band structure analyses and applications. However, accurate measurements of optical constants for a biaxial material are known to be very difficult.

<u>In this work:</u>

We report the results of the polarized transmission intensity (PTI) and spectroscopic ellipsometry (SE) measurements of principal components of the dielectric function tensor of biaxial $CaGa_2S_4$ using (100)-oriented surface plane.

Structure and symmetry of CGS

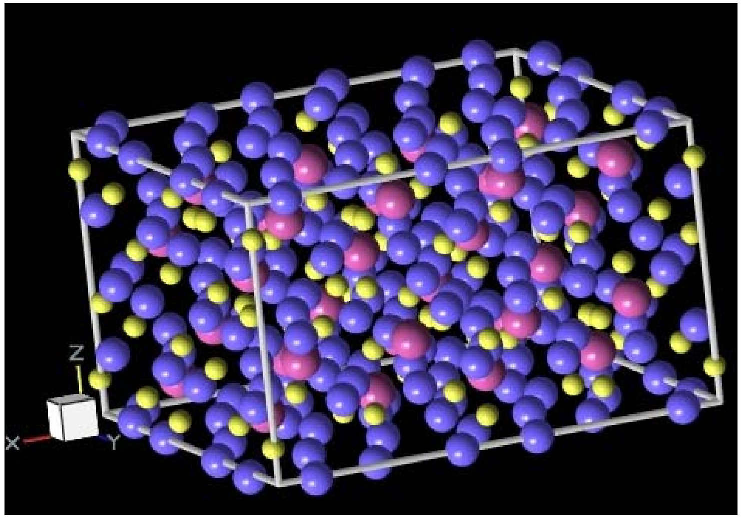

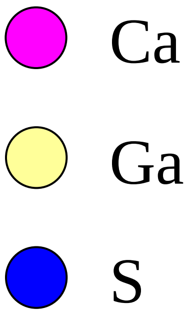

- Space group*
  D_{2h}^{24} (Fddd)
  Orthothombic
- Lattice constants*
  a=21.06Å
  b=21.00Å
  c=12.66Å

* G.G. Guseinov, F. Kh. Mamedov, I.R. Amiraslanov, Kh. S. Mamedov: Crystallography, 28 (1983) 866.

- **Optical anisotropy**
  Biaxial crystal
- **Cleavage plane**
  (100) plane
- **Energy gap**
  4.1eV (R.T.)

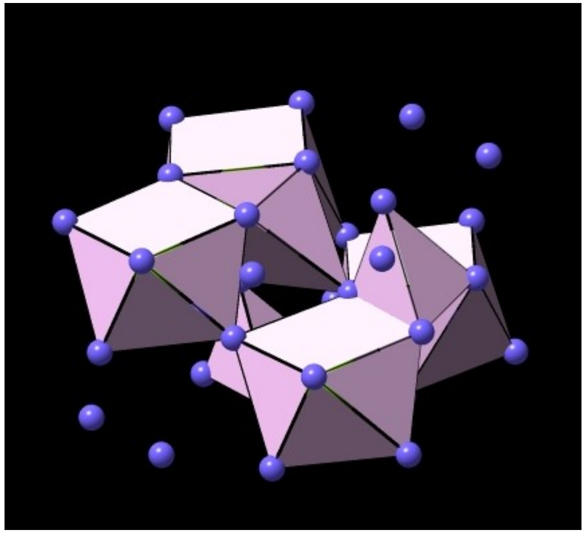

Strategy for determination of optical constants of biaxial CGS

We need 2 or 3 different crystal faces to obtain optical constants of biaxial CGS by using conventional biaxial ellipsometry technique.

↓

But we can prepare only (100) surface for SE measurement.

↓

To obtain principal optical constants from only (100) crystal surface,
We have to analyze separately two energy regions.

Below the band gap energy region

Effective value of refractive indices were measured by PTI method.

→

The obtained effective values were optimized by comparison with SE data.

Above the band gap energy region

Analytical approximation approach to biaxial materials was used.
(This approach is effective in case of rather large values of dielectric function.)

PTI set-up (for analysis below the band gap energy region)

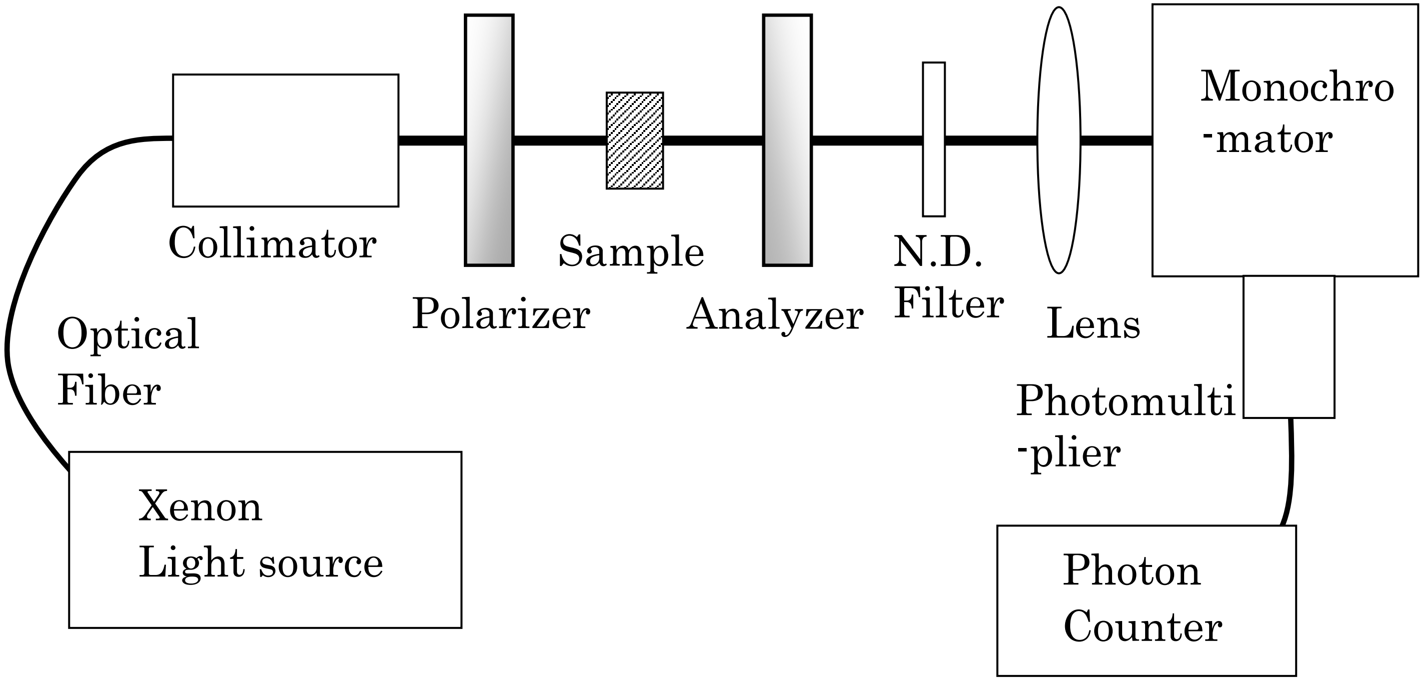

Experimental set-up for polarization transmission intensity (PTI) measurements.

PTI data on CGS

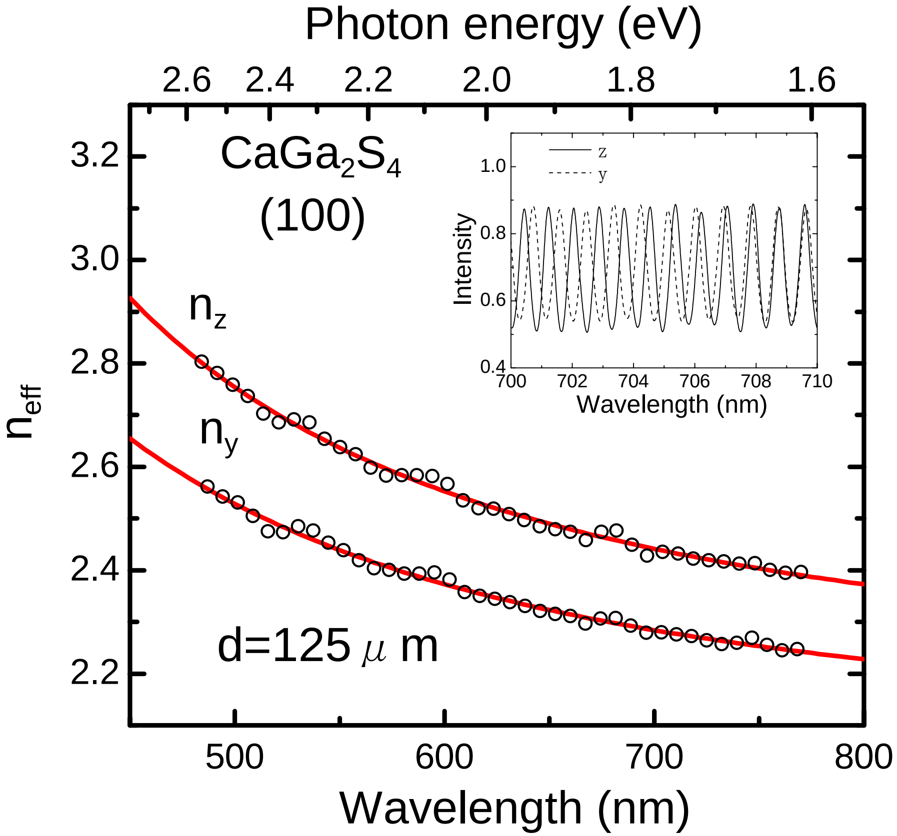

The effective values of refraction indices determined from interference fringe separation in PTI spectra. Inset: Fringe pictures obtained for z and y components.

○Determination of effective refractive indices from interference fringe

$$n_{eff} = \frac{\lambda_{m+\Delta m}\lambda_m}{\lambda_m - \lambda_{m+\Delta m}} \times \frac{1}{2d} \times \Delta m$$

Obtained results are only effective values.

We have to correct these results by comparison with ellipsometric results.

Optimization of obtained refractive indices by SE measurement

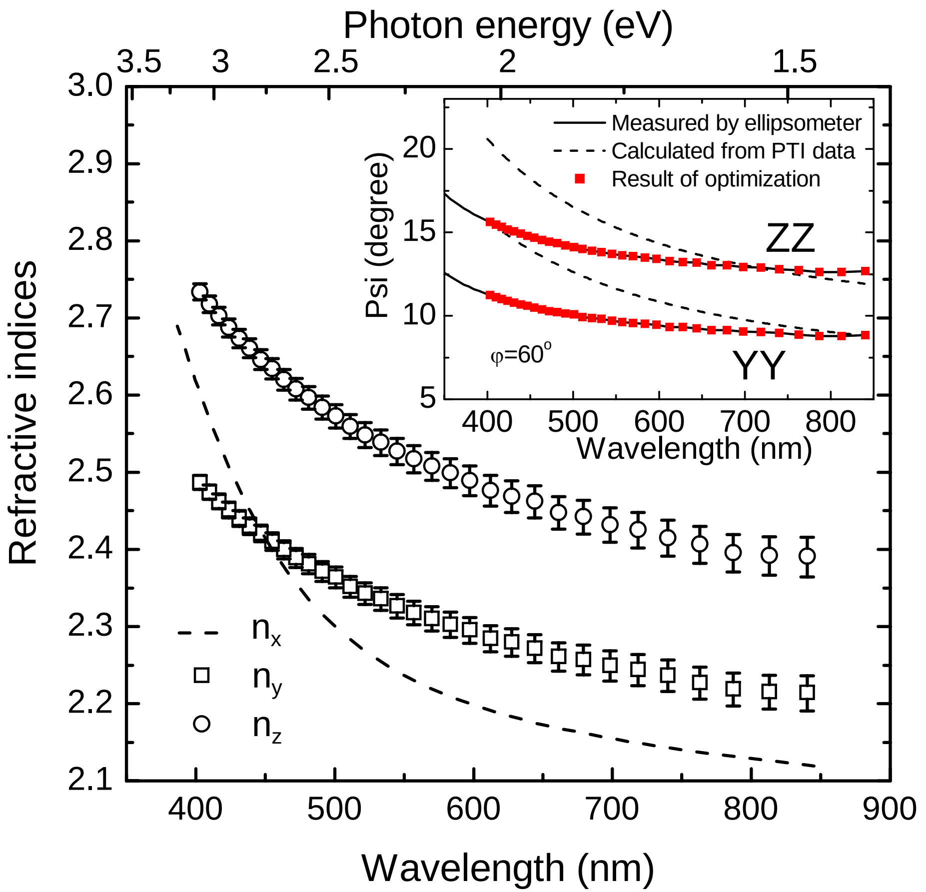

Optimized refraction indices. Inset: Comparison of the experimental ψ with that calculated using optimized values of refraction indices.

○ Optimization of refractive indices was done by minimizing error function G*

$$\rho = \frac{r_{pp}}{r_{ss}} = \tan \psi e^{i\Delta}$$

$$G(\bar{n}_x, \bar{n}_y, \bar{n}_z) = \sum_{\delta = zz, yy} \{[\mathrm{Re}(\rho_\delta^{meas}) - \mathrm{Re}(\rho_\delta^{calc})]^2 + [\mathrm{Im}(\rho_\delta^{meas}) - \mathrm{Im}(\rho_\delta^{calc})]^2\}$$

ρ_δ^{meas} : measured by ellipsometry

ρ_δ^{calc} : calculated from PTI results

δ : configuration (YY or ZZ)

*S. Logothetidis, M. Cardona, P. Lautenschlager, M. Garriga, Phys. Rev. B 34 (1986) 2458.

Above-energy-gap SE data on CGS

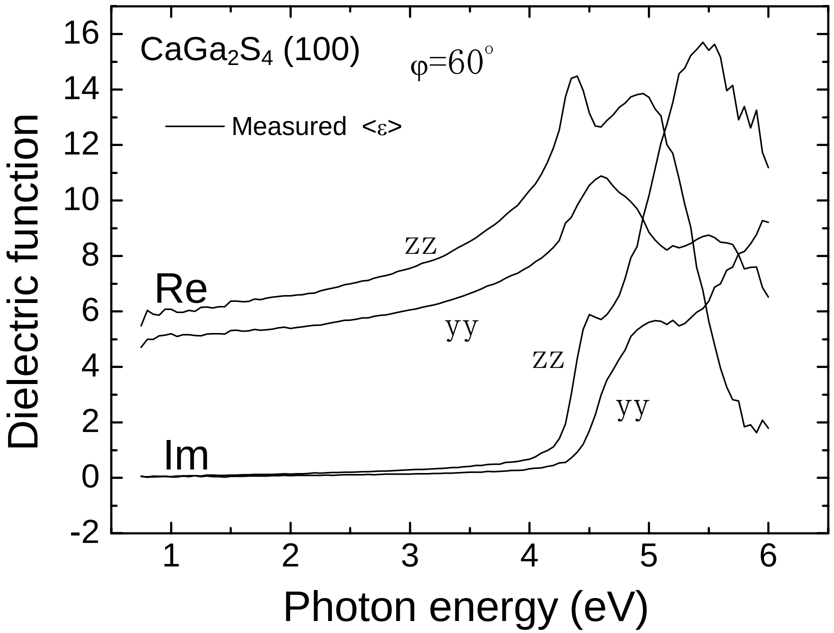

Pseudo-dielectric function spectra of $CaGa_2S_4$ measured for YY and ZZ configurations on (100) surface.

We have to restore the principal components of dielectric function from these results by analytical treatment for biaxial materials.

YY configuration

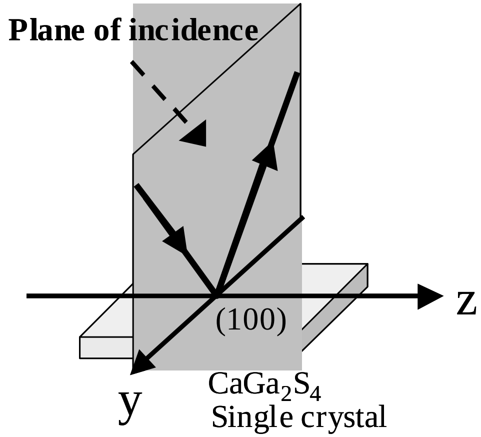

ZZ configuration

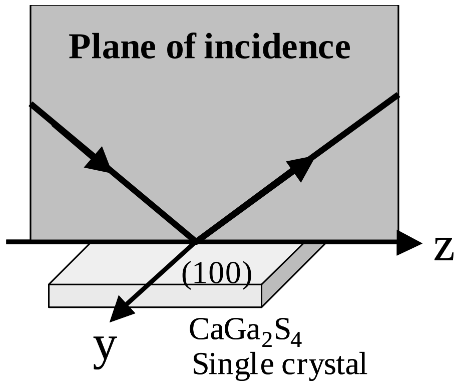

Results of analytical treatment

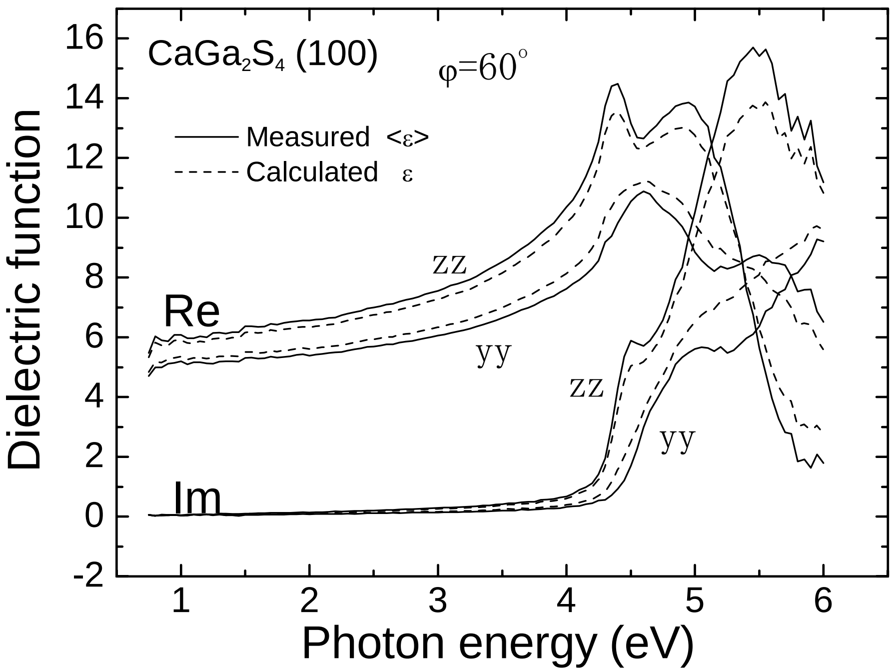

Measured pseudo-dielectric function (solid line) and analytically treated (broken line) spectra for $CaGa_2S_4$ with the ZZ and YY configuration.

We have a problem in the results of this analytical approach. Because this approach is effective in case of rather large values of dielectric function.

Incident angle dependency

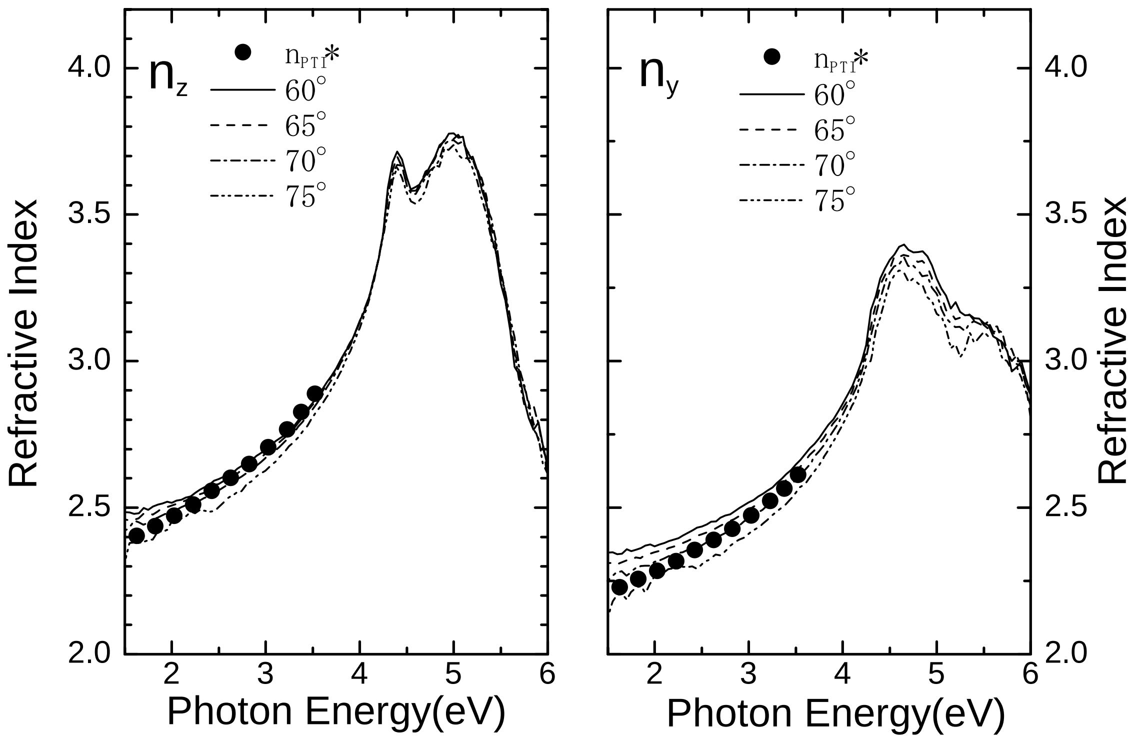

Incident angle dependence of obtained optical constants with result of PTI measurement.

In the region above energy gap (>4.1eV), the optical constants obtained from each incident angles show good agreement.

In the region below energy gap (<4.1eV), the large angle dependency is observed in the obtained optical parameters.

Because values of dielectric function are rather small.

PTI results are adopted to the optical constants of CGS in the region below energy gap.

Finalized form of principal components of dielectric function

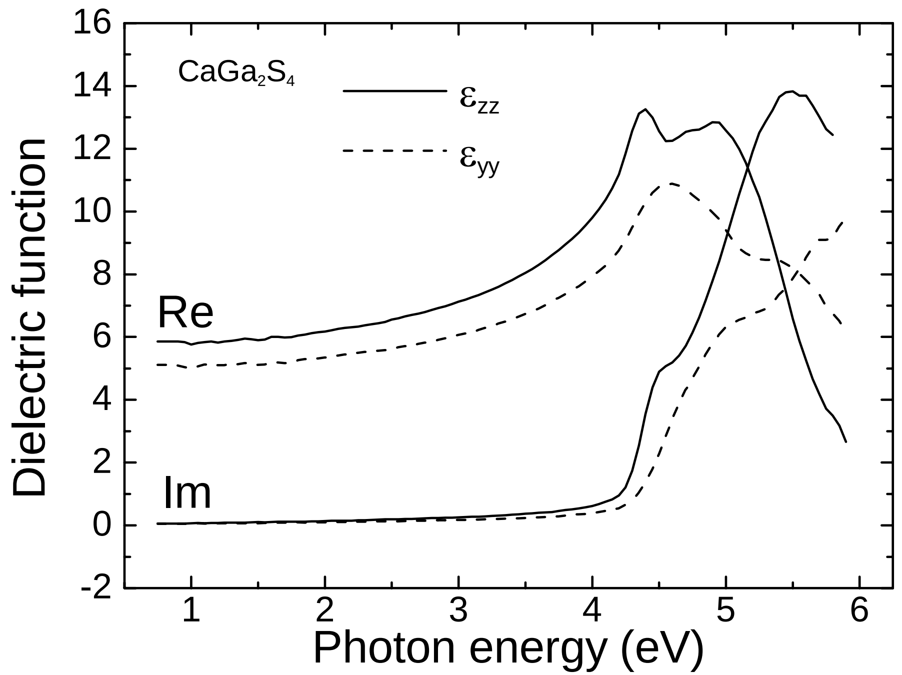

Real and imaginary parts of the principal components of the dielectric function of $CaGa_2S_4$.

If we adopt PTI obtained optical constants as true optical constants then we can introduce corrections into dielectric function over the all accessed energy region and get most trustable dielectric functions. So the results of such a procedure are shown in this figure.

Summary on $CaGa_2S_4$

For the first time,

- CGS samples with (100) surfaces have been studied by PTI and SE, and the major refraction indices have been determined in the region below the energy gap.
- The principal components, zz and yy, of the dielectric function of CGS have been obtained in the spectral range 0.75-6.00eV by using conventional biaxial SE approach to the experimental ellipsometric data.

III. Incoherent ellipsometry on depolarizing samples ($TlMeX_2$)

- Background
- Structure and symmetry of layered $TlMeX_2$ ($TlInS_2$, $TlGaSe_2$ and $TlGaS_2$)
- About spectroscopic phase modulated ellipsometry (SPME)
- SPME measurements on layered anisotropic materials
- Incoherent reflection model
- Results and discussion
- Summary on $TlMeX_2$

Background

- Quasi-two-dimensional layered $TlInS_2$, $TlGaS_2$ and $TlGaSe_2$ ($TlMeX_2$) exhibit paraelectric(P) - incommensurate(I) - ferroelectric(F) structural phase transition with decreasing the temperature.
- The optical properties of the $TlMeX_2$ with the nano-scale spatial modulation emerging in the I-phase are very attractive from the point of view of both the underlying physics* and optical memory device applications**.
- In a recent work***, increasing of biaxial anisotropy of $TlInS_2$ in I-phase was observed by using light figure technique.

In this work we have examined the $TlMeX_2$ to obtain refractive index of this material both in E//c* and E⊥c* orientations at room temperature in a region below the energy gap by using spectroscopic phase modulated ellipsometry (SPME).

* N. Mamedov, T. Aoki-Matsumoto, B. Gadiev, H. Uchiki, N. Yamamoto, S. Iida: *Proc. 25th Int. Conf. Semiconductor Physics, Osaka, 2000* (Springer-Verlag, Heidelberg, 2001) p.123.

** H. Uchiki, D. Kanazawa, N. Mamedov, S. Iida, J. Luminescence **87-89** (2000) 664.

*** Y.Shim, W. Okada, N. Mamedov, Thin Solid Films, to be published.

Structure and symmetry of layered $TlMeX_2$ ($TlInS_2$, $TlGaSe_2$ and $TlGaS_2$)

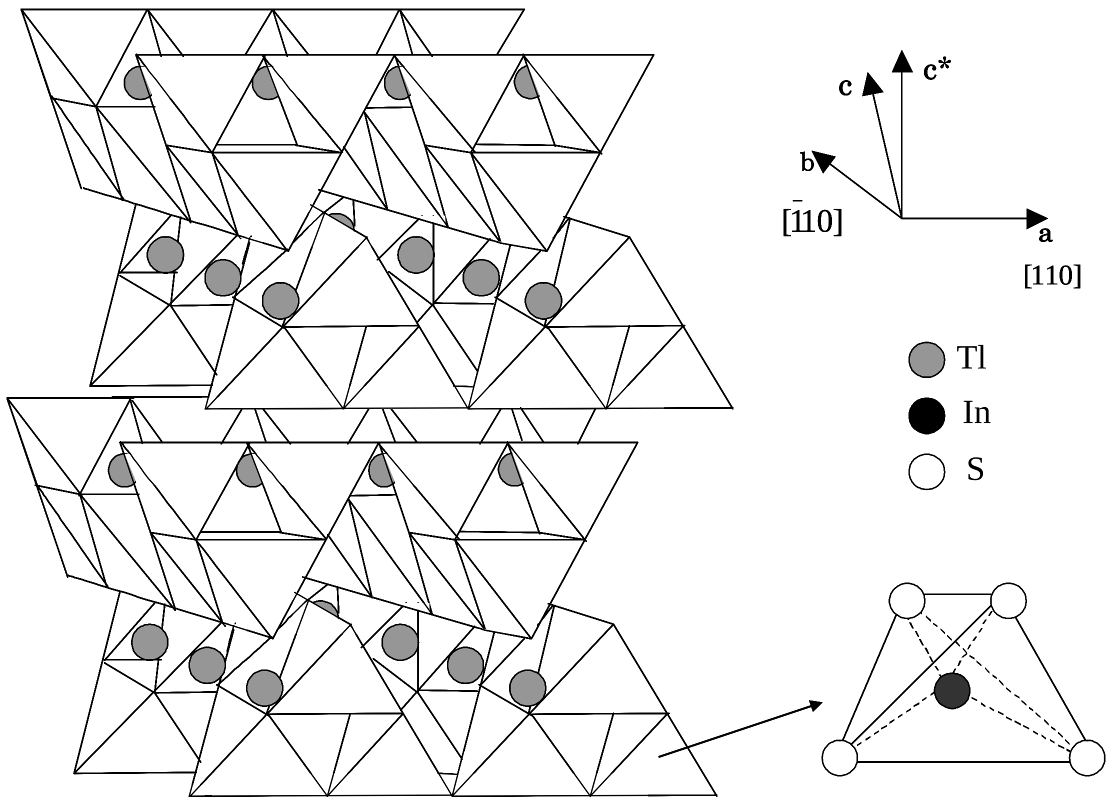

Crystal structure of $TlInS_2$ ($TlGaS_2$ and $TlGaSe_2$ have same structure).

- Layer plane

  Normal to c*: (001)

- Space group

  C_{2h}^{6} (R.T.)

- Optical anisotropy

  Biaxial crystal

Biaxial (in-layer-plane) anisotropy is three orders of magnitude smaller than anisotropy across the layers*.
Therefore we can treat $TlMeX_2$ as uniaxial material with optic axis normal to the layer plane.

* N. Mamedov, Y. Shim, N. Yamamoto, Jpn. J. Appl. Phys. **41** (2002) 7254.

About SPME

Spectroscopic Phase-Modulated Ellipsometer (SPME)

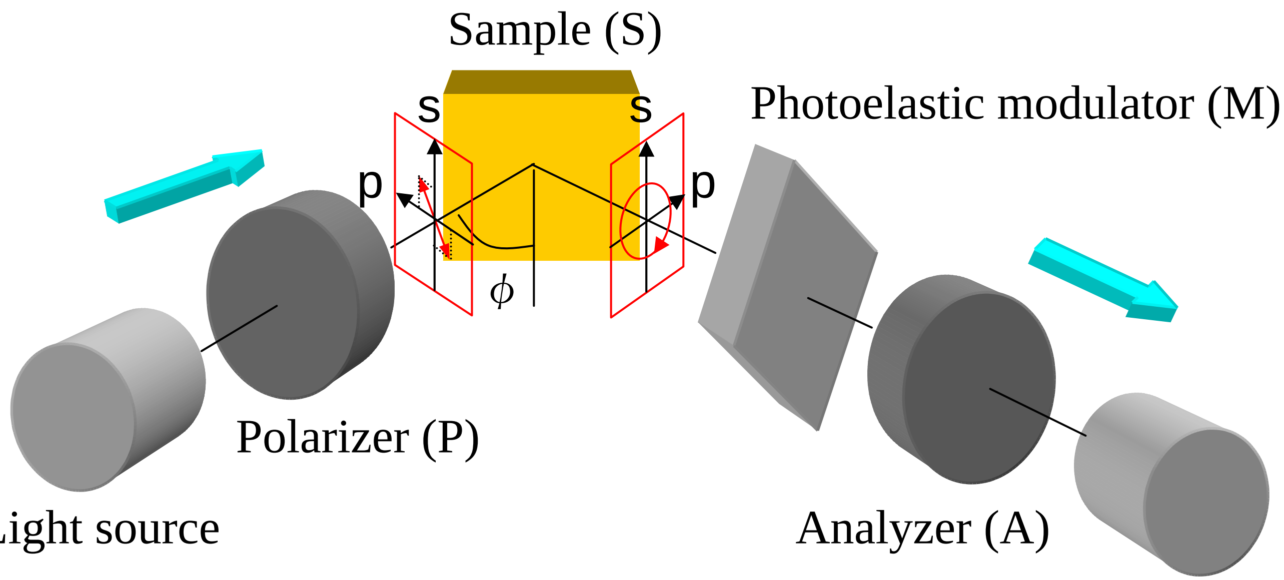

The optical configuration of SPME.

Measured intensity

$$I(t) = I_0\{1 + Is[2J_1(F)\sin\omega t] + Ic_2[2J_2(F)\cos 2\omega t]\}$$

$$Is = \sin(2\psi)\sin(\Delta) \qquad Ic_2 = \sin(2\psi)\cos(\Delta)$$

$$\rho = \frac{r_{pp}}{r_{ss}} = \tan\psi \cdot e^{i\Delta}$$

SPME measurements on layered anisotropic materials

- In the case of a layered material, preparation of two main crystal faces having same high-grade optical quality is quite difficult and in most cases only layer-plane crystal face is available for measurements. In the measurement for layered Tl compounds we can use only the surface normal to c* axis.
- In SE measurements using coherent reflection model, the restoration of the refractive index from the measurements on the layer plane surfaces of a layered material in E//c* configuration is quite difficult because of the small contribution of the E//c* component into total reflection.

Here we use an incoherent reflection model for ellipsometric analysis, which is much more sensitive to the anisotropy of the refractive indices because of the interference effect.

Incoherent reflection model*

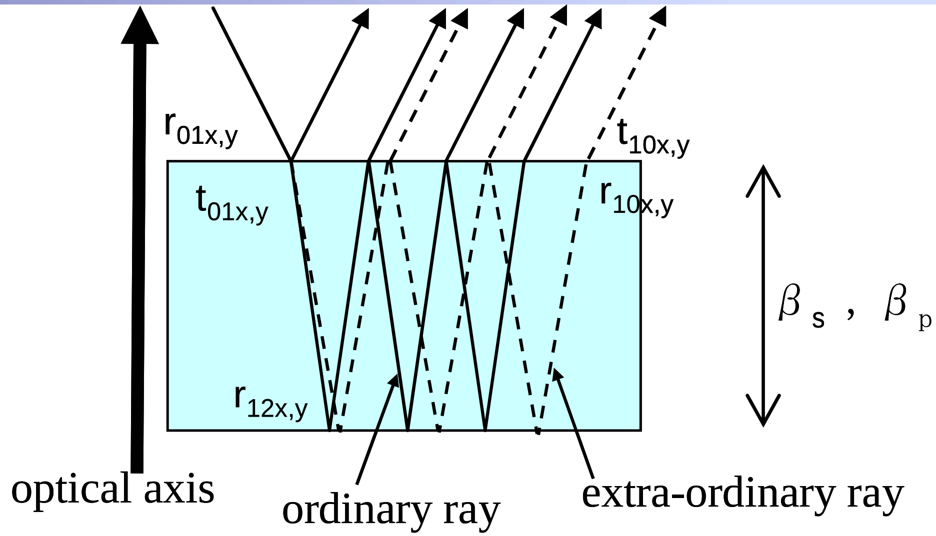

Reflection and transmission from uniaxial plate.

If the sample has thickness of the order of several micrometers, we will have an interference effect and SE spectra will be fringe type because of the interference between ordinary and extraordinary rays.

$$\langle r_x r_y^* \rangle = r_{01x} r_{01y}^* + \frac{(t_{01x} t_{01y}^*)(t_{10x} t_{10y}^*)(r_{12x} r_{12y}^*)\exp[2i(\beta_x - \beta_y^*)]}{1 - (r_{10x} r_{10y}^*)(r_{12x} r_{12y}^*)\exp[2i(\beta_x - \beta_y^*)]}$$

$$Is \equiv \gamma = \frac{2\,\mathrm{Im}\,\langle r_p r_s^* \rangle}{\langle r_s r_s^* \rangle + \langle r_p r_p^* \rangle}$$

$$Ic_2 \equiv \beta = \frac{2\,\mathrm{Re}\,\langle r_p r_s^* \rangle}{\langle r_s r_s^* \rangle + \langle r_p r_p^* \rangle}$$

$$\beta_s = 2\pi \frac{d}{\lambda}\left(n_o^2 - n^2 \sin^2 \varphi_0\right)^{1/2} \qquad \beta_p = 2\pi \frac{d}{\lambda}\frac{n_o}{n_e}\left(n_e^2 - n^2 \sin^2 \varphi_0\right)^{1/2}$$

* R. Ossikovski, M. Kildemo, M. Stchakovsky,and M. Mooney, Applied Optics, **39** (2000) 2071.

Results and discussion

➢ $TlInS_2$

Experimental conditions

- Sample : **$TlInS_2$** single crystal
  (Thickness 210 μm)
  both sides cleaved surfaces
- Incident angle : 56°

Fitting conditions

- Dispersion model
  n_e : Sellmeier model
  n_o : Obtained from bulk-$TlInS_2$
- Fitted energy region : 0.8-2.2eV

Sellmeier model

$$n_e^{\,2} = n_{se}^{\,2} + \frac{f_{se}E_{se}^{\,2}}{E_{se}^{\,2} - E^2}$$

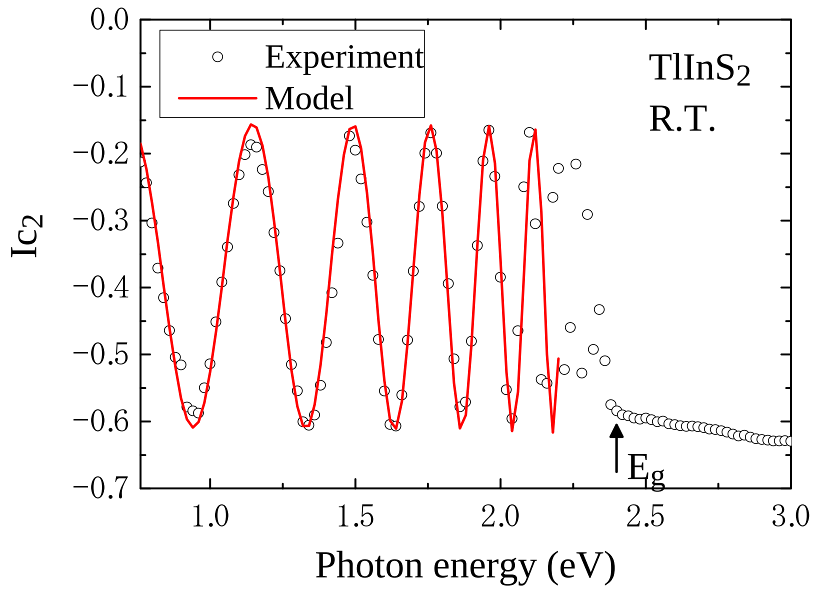

SPME *Ic* signal as a function of photon energy for $TlInS_2$ plate at room temperature. The band gap energy (2.4eV) of $TlInS_2$ is indicated by arrow.

Obtained optical constants of $TlInS_2$

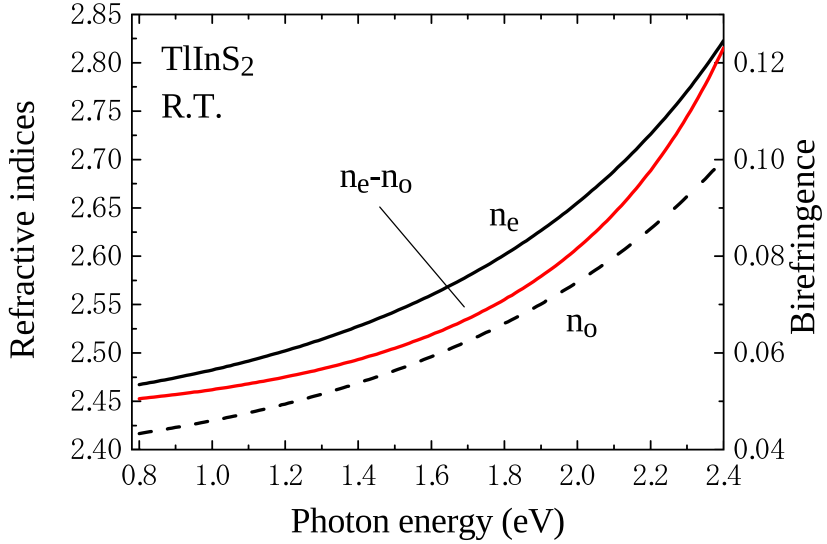

Refractive indices n_o(E⊥c*), n_e(E//c*) and uniaxial birefringence, n_e-n_o, as obtained for $TlInS_2$ by using incoherent ellipsometric approach.

- $TlInS_2$ can be regarded as optically positive material. It is consistent with the optical polarizing microscope data. The uniaxial optical anisotropy is found to be large, agreeing well with that of ∼0.1 reported earlier*.
- Uniaxial anisotropy of $TlInS_2$ is a steeply increasing function of photon energy in the region near the absorption edge at 2.4eV.

* N. Mamedov, Y. Shim, N. Yamamoto, Jpn. J. Appl. Phys. **41** (2002) 7254.

Anisotropic optical constants near the band edge

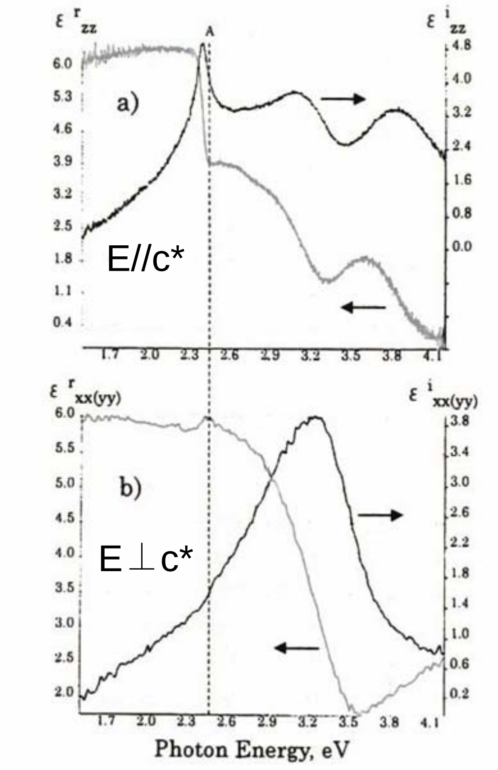

Real and imaginary parts of dielectric function spectra of $TlInS_2$ at room temperature for (a) E//c* and (b) E⊥c* configurations by using coherent reflection model*

The strong dispersion of birefringence near the absorption edge at 2.4eV.

This fact definitely confirms the results shown in figure according to which band gap exciton transitions are allowed in E//c* and forbidden in E⊥c* orientation.

* N. Mamedov, *et al.*： : *Proc. 25th Int. Conf. Semiconductor Physics,Osaka, 2000* (Springer-Verlag, Heidelberg, 2001) p.123.

Refractive indices of $TlGaS_2$ and $TlGaSe_2$

➢ $TlGaS_2$ and $TlGaSe_2$

- Sample : **$TlGaS_2$** single crystal
  (Thickness 165 μm)
  $TlGaSe_2$ single crystal
  (Thickness 340 μm)
- Incident angle : 60°
- Fitted energy region : **$TlGaS_2$** 0.8-2.4eV
  $TlGaSe_2$ 0.8-2.0eV

➢ **$TlGaS_2$**、 **$TlGaSe_2$** : $n_e > n_o$

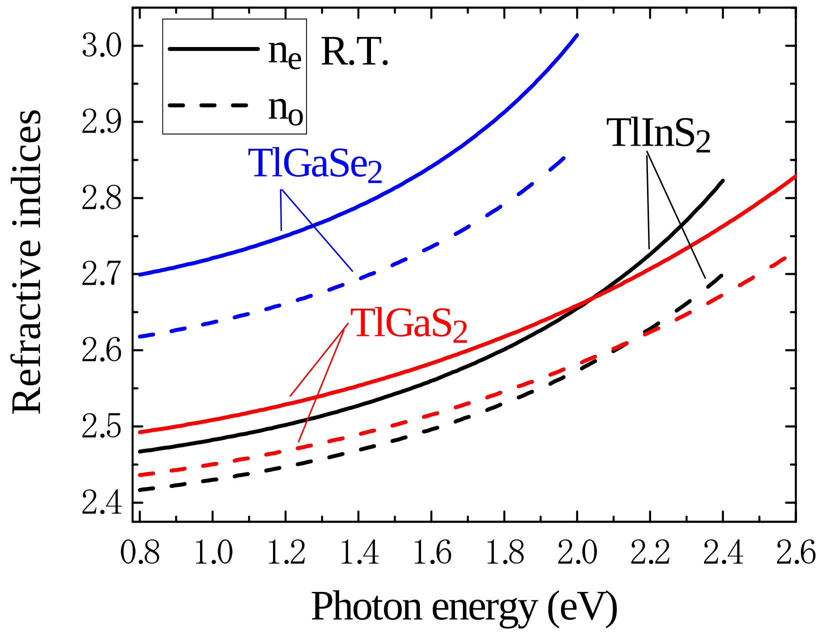

Birefringence of $TlGaS_2$ and $TlGaSe_2$

- Absolute value of birefringence
  - All compounds : ~ 0.1

This result is consistent with the reported value obtained from light figure spectroscopic measurements*.

- Dispersion of birefringence
  - **$TlGaSe_2$**

Birefringence of $TlGaSe_2$ shows strong dispersion same as $TlInS_2$. We can expect that $TlGaSe_2$ has strong absorption allowed in only E//c* orientation.

  - **$TlGaS_2$**

Birefringence of $TlGaS_2$ shows not so strong dispersion in comparison with the other two compounds.

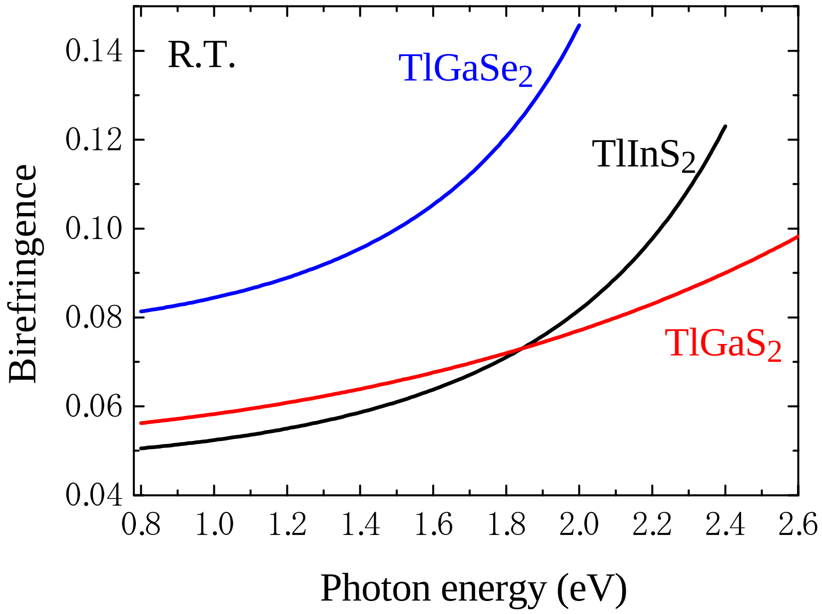

*N. Yamamoto, *et al.*: J. Crystal Growth, **237/239** (2002) 2023.

Summary on $TlMeX_2$

- By applying the incoherent ellipsometric approach and uniaxial approximation to SPME data obtained for only one, layer-plane crystal face of $TlInS_2$, $TlGaS_2$ and $TlGaSe_2$ samples at room temperature, we have determined the spectral dependencies of the refractive indices, n_o and n_e, of this material in E⊥c* and E//c* orientations, respectively.
- The obtained results are entirely consistent with the reported fact that band gap exciton transitions in $TlInS_2$ and $TlGaSe_2$ at room temperature are allowed in E//c* and forbidden E⊥c* orientation.

IV. Summary of this presentation

- Spectroscopic ellipsometry on moderate and wide gap materials for which ellipsometric measurements can already be done in the region below the energy gap is a powerful tool for anisotropic materials characterization even if only one high grade sample surface is available for measurements.
- As persuasive examples we have demonstrated our results obtained for biaxial CGS and $TlMeX_2$ by using coherent and incoherent ellipsometric approaches, respectively.